American Chemical Society: Environmental Science & Technology: Water (*ACS EST Water*)
Volume 1, Issue 2, December 2020, pp. 376-387
DOI:10.1021/acsestwater.0c00145

Aquatic macrophytes in morphological and physiological responses to the nanobubble technology application for water restoration

Shuo Wang, Yunsi Liu, Tao Lyu, Gang Pan*, Pan Li*

AUTHOR INFORMATION

Corresponding Authors

Pan Li − *State Key Laboratory of Control and Resource Reuse, School of Environmental Science and Engineering, Tongji University, 1239 Siping Road, Shanghai, PR China;* orcid.org/0000-0002-5192-8509; E-mail: lipan@tongji.edu.cn

Gang Pan − *Integrated Water-Energy-Food Facility (iWEF), School of Animal, Rural, and Environmental Sciences, Nottingham Trent University, Nottinghamshire NG25 0QF, UK;* orcid.org/0000-0003-0920-3018; E-mail: gang.pan@ntu.ac.uk

Authors

Shuo Wang − *School of Environmental Science and Engineering, Tongji University, 1239 Siping Road, Shanghai, PR China;* orcid.org/0000-0002-2072-2962

Yunsi Liu − *School of Environmental Science and Engineering, Tongji University, 1239 Siping Road, Shanghai, PR China;* orcid.org/0000-0002-6315-7705

Tao Lyu − *Cranfield Water Science Institute, Cranfield University, College Road, Cranfield, Bedfordshire, MK43 0AL, UK;* orcid.org/0000-0001-5162-8103

Abstract

Nanobubble technology, as an emerging and sustainable approach, has been used for remediation of eutrophication. However, the influence of nanobubbles on the restoration of aquatic vegetation and the mechanisms are unclear. In this study, the effect of nanobubbles at different concentrations on the growth of *Iris pseudacorus* (*Iris*) and *Echinodorus amazonicus* (*Echinodorus*) was investigated. The results demonstrated that nanobubbles can enhance the delivery of oxygen to plants, while appropriate nanobubble levels will promote plant growth, excess nanobubbles could inhibit plant growth and photosynthesis. The nanobubble concentration thresholds for this switch from growth promotion to growth inhibition were 3.45×10^7 and 1.23×10^7 particles/mL for *Iris* and *Echinodorus*, respectively. Below the threshold, an increase in nanobubble concentration enhanced plant aerobic respiration and ROS generations in plants, resulting in superior plant growth. However, above the threshold, high nanobubble concentrations induced hyperoxia stress, particularly in submergent plants, which result in collapse of the antioxidant system and the inhibition of plant physiological activity. The expression of genes involved in modulating redox potential and the oxidative stress response, as well as the generation of relevant hormones, were also altered. Overall, this study provides an evidence-based strategy to guide the future application of nanobubble technology for sustainable management of natural waters.

Keywords: Eutrophication control; Oxidant/antioxidant species; Chlorophyll content; Gene expression; Hormone generation

Synopsis

Our study provided an evidence-based strategy to guide the future application of nanobubble technology for sustainable management of natural waters.

Published by American Chemical Society. This is the Author Accepted Manuscript issued with: Creative Commons Attribution Non-Commercial License (CC:BY:NC 4.0). The final published version (version of record) is available online at DOI:10.1021/acsestwater.0c00145. Please refer to any applicable publisher terms of use.

1. Introduction

Nanobubbles are defined as bubbles with a diameter of less than 1000 nm with special characteristics resulting from their ultra-fine size[1]. Compare with the rapid and high gas transfer efficiency of microbubbles (bubble size in micrometres), the gas dissolution speed would be much slower/sustainable, e.g. increase the DO in the water, for nanobubbles due to the longer lifetime and lower buoyancy. Additionally, the natural collapse of nanobubbles could generate reactive oxygen species (ROS), including hydroxyl radicals ($^{\bullet}OH$), superoxide radicals ($^{\bullet}O_2^-$), and singlet oxygen ($^1O_2$).[2] Previous studies have also shown that micro/nanobubbles can improve the lysis of harmful algal cells and the detoxification of cyanotoxins.[3] Therefore, bulk micro/nanobubbles have been directly exploited to remove aerobically degradable pollutants (e.g., organic waste and ammonium) and harmful algal blooms (HABs) from eutrophic waters.[4,5] Alongside the use of bulk nanobubbles, a novel refinement of the technology, which involves interfacial nanobubbles, was developed in 2018, using natural minerals loaded with oxygen to deliver oxygen nanobubbles onto sediment surfaces.[6,7] This approach successfully reversed sediment hypoxia and reduced the flux of N and P from the sediment for over four months. Therefore, there has been increasing research interest and deployment on nanobubble technology for the in-situ control of eutrophication. Many companies in Asia, the US and Europe have become increasingly involved in projects that use nanobubble technology for HAB mitigation.[3,8,9] Nevertheless, both bulk and interfacial nanobubble treatments have mainly focused on the first step of water restoration, i.e. pollutant removal and sediment remediation. After the pollutants removal to a certain level along with the water quality improvement, the clear-water state in natural waters could offer a satisfactory situation for the restoration of aquatic vegetation in the later stage. Since the nanobubble technology operation time and nanobubble concentrations have not been

precisely regulated, the potential impact of nanobubbles on the later processes of aquatic vegetation growth and stabilisation is still unclear.

As an important part of the aquatic ecosystem, aquatic vegetation provides a variety of important ecological services, including improving water clarity, stabilising sediments and providing food and habitats for aquatic animals.[10] Unlike terrestrial plants, aquatic plants, particularly when fully submerged, are more likely to face problems of oxygen limitation. Reduced availability of oxygen for cell respiration is likely to limit energy production and negatively influence plant growth.[11] Nanobubbles, which have superior oxygen/air transfer efficiency, are expected to assist aquatic vegetation to overcome such oxygen shortages; indeed, they have been used to improve plant seed germination,[12] biomass growth (e.g., lettuce and spinach)[13,14] and crop yield (e.g., tomato)[15]. Moreover, it is reported that the nanobubbles in the water can stimulate endogenous ROS generation inside plants.[16,17] An appropriate ROS level is required to activate plant proliferative pathways,[18] and thus they can be considered to promote plant growth.[16,17] Therefore, it is hypothesised that the presence of the nanobubbles during the water restoration could not only removal the pollutants but also benefit the aquatic plants restoration.

However, as applied to water restoration, the parameters of nanobubble technology, such as the appropriate operation time and nanobubble concentrations, have not been precisely defined. This is important because excess oxygen and ROS levels are likely to result in oxidative damage that could overwhelm the plant's oxidative stress response and negatively impact its metabolism.[19] Indeed, intermittent micro/nanobubble aeration has been shown to cause oxidative damage to the root tip cells and thereby inhibit the growth of spinach plants.[20,21] Liu et al (2016) also reported that the exogenous hydroxyl radicals (·OH)

resulting from high levels of nanobubbles in water decreased hypocotyl elongation and chlorophyll formation in carrot and spinach.[16] Furthermore, in our previous research, we found that the submergent plant, *Echinodorus amazonicus*, gained 25% less biomass in micro/nanobubble-aerated water compared with plants aerated by macrobubbles, even with similar dissolved oxygen (DO) levels.[22] Nevertheless, we hypothesise that the emergent aquatic plants, which dominate the vegetation of most shallow lakes and wetlands, may have a higher tolerance of nanobubbles as the majority of the plant biomass is above water level, but this has never been examined in detail. Therefore, a quantitative investigation of the effect of nanobubbles on the growth of both emergent and submergent aquatic plants will be crucial as a guide to the application of nanobubble technology to water restoration. It is further hypothesised that the plant physiological response, in terms of oxidant/antioxidant species generation, hormone production and gene expression, would be different for emergent and submergent aquatic plants.

In this study, *Iris pseudacorus* (*Iris*) and *E. amazonicus* (*Echinodorus*) were selected as examples of indigenous emergent and submergent aquatic vegetation, respectively. The sediment and water were collected from a light-eutrophic reservoir as a growth medium for both plant species, which were then subjected to different nanobubble concentrations (10^6-10^8 particles/mL). DO concentrations were kept at a similar level in plant cultures to investigate the effect of a single factor (i.e. nanobubble concentration). Plant morphology, e.g. biomass, root/leaf length and chlorophyll content, were monitored to evaluate the effect of nanobubbles on plant growth. We also assessed the characteristics of plant physiology, including oxidant/antioxidant species generation, gene expression patterns and hormone production, to reveal the mechanisms of the plant response to nanobubble treatment. Overall,

this study aimed to obtain the threshold nanobubble levels that support the growth of aquatic vegetation and provide evidence-based results to underpin the application of nanobubble technology to natural water restoration.

2. Experimental Section

2.1 Aquatic plant preparation and in-situ collection of sediment and water

Water and sediment/soil were collected from a light-eutrophic reservoir with surface area 2.7 km^2 and average water depth 3 m. The concentrations of total nitrogen and total phosphate in the water were around 1.05-2.27 and 0.06-0.16 mg/L, respectively. Algal blooms occur in the reservoir every summer with an algal density as high as 10^7 cells/mL. Nanobubble aeration was applied at the entrance of the reservoir, and subsequently combined with wetland areas. The sediment/soil samples were collected from the upstream of the reservoir, which located around 1.2 km from the entrance. *Iris* and *Echinodorus* are both prevalent native plants; seedlings of both species were bought from a local horticultural company (Rongyue Ltd., Shanghai, China). The initial height of the *Iris* was around 10 cm and the initial weight of the *Echinodorus* was around 20 g.

2.2 Experimental setup and operation

Iris and *Echinodorus* were cultivated at room temperature (25 ± 5℃) with a 10 h photoperiod per day (LED plant lamps, photosynthetic photon flux density 180 μmol m^{-2} s^{-1}, 150D, GAKO, China). *Iris* was cultivated hydroponically to simulate the floating bed system and subsequent constructed wetlands in this reservoir, which was grown in a polymethyl methacrylate tank with dimensions 55 × 18 × 30 cm in groups of 16 seedlings. Emergent seedlings were inserted into the holes of a styrofoam plate floating on water and cultivated for 21 days. *Echinodorus* was grown in polymethyl methacrylate cylinders with an inner

diameter of 35 cm and a height of 40 cm. Each cylinder contained three plant clusters. Submergent seedlings were cultivated in sediment for 40 days. Surface water (20 L) from the reservoir was used in each tank or column. All plants were stabilised for three days prior to the experiment.

The water condition was set to simulate the late stage of the nanobubble eutrophication remediation process. For both emergent and submergent plants, six parallel groups were prepared to investigate the effects of different nanobubble concentrations on plant growth. Each group had three replicates. The system without aeration treatment was set up as the control group. In the macrobubble (MAB) aeration group, normal air pump was conducted continuously (Table 1). To achieve such different nanobubble concentrations, two most common methods, i.e. pressurisation and cyclone shear methods, were used in this experiment. It has been documented that there is no difference in the physicochemical properties of nanobubbles generated by the two methods except particle size and concentration[20]. The intermittent nanobubble aerations and coupled with dilution method were conducted in the nanobubble (NB) aeration groups (Table 1), which were categorized as low, medium, high and super-high NB groups according to different concentrations of nanobubble in the water.

2.3 Nanobubble distribution and water quality measurement

Each nanobubble aeration treatment was conducted in pure reservoir water with air as the gas source to simulate the experimental conditions before plant cultivation. Nanobubble size distribution (<1000 nm) from all groups were measured right after the intermittently aeration and/or dilution by dynamic light scattering using a NanoSight NS3000 instrument (Malvern Panalytical, UK). Each measurement was replicated three times. During the

experiment, temperature, pH, DO levels of the water in all groups were measured every two days using a YSI 556 multi-parameter system (Xylem Inc., USA). To avoid cross-contamination, the probes were carefully cleaned with ultrapure water between measurements.

Table 1

Experimental conditions and aeration methodologies in different groups.

Group	Aeration	Method and Instrument	Energy consumption
Control	No aeration	-	0
MAB	Continuously aeration	Air pump and porous diffuser (YTZ-312, YEE, 3W, China)	150 W/m^3
L-NB	0.4 L water was taken out daily for 2-min aeration and replenishment	Pressurisation method (LF-1500, XINGHENG, 0.4L/min, 90W, China)	6.25 W/m^3
M-NB	4 L water was taken out daily for 10-min aeration and replenishment	Pressurisation method (LF-1500, XINGHENG, 0.4L/min, 90W, China)	31.25 W/m^3
H-NB	1-min aeration / 30 min	Cyclone shear method (Ubble-ed2.0, XINGHENG, 4 L/min,100W, China)	166.67 W/m^3
S-NB	1-min aeration / 30 min	Pressurisation method (MF-5000, XINGHENG, 4 L/min, 500W, China)	833.33 W/m^3

MAB, L-NB, M-NB, H-MB, S-NB represent macrobubble aeration, low, medium, high and super-high nanobubble aeration groups, respectively.

2.4 Plant morphological and physiological responses

2.4.1 Plant growth

At the end of the experiment, all plants were harvested and the fresh weight, root/leaf length and chlorophyll content (HACH®, DR 6000, USA) were measured. The transplanting-survival rates (the percentage of plants that was alive after 7 days) and biomass growth ratios (the ratio of the final fresh weight divided by the initial fresh weight) were calculated for the comparison between groups. Other measured parameters were based on

the survived plants, which could avoid the bias of the initial stabilisation differences that wouldn't happen in the real application.

2.4.2 Oxidant and antioxidant species

For each species of plant, 5 g tissue samples were taken randomly from leaves and roots; samples were mechanically homogenized in phosphate buffer at a mixing ratio of 1:9 (w/v) on ice. The suspension was then centrifuged for 5 min at 12000 rpm at 4℃. In the presence of superoxide radical, hydroxylamine is oxidized to nitrite, which can be determined by adding 1 ml each of 17 mM sulphanilic acid and 7 mM 1-naphthalene acetic acid solutions to 1 ml reaction mixture. The components were mixed and after being left at room temperature for 20 min, A_{530} was measured to calculate the concentration of superoxide radical.[23,24]

The total antioxidant capacity (T-AOC) was measured with a T-AOC assay kit (colorimetric method, A015, Nanjing Jiancheng Bioengineering Institute). The buffer solutions, ABT solution, peroxide solution, Trolox solution and samples were then prepared according to the manual of the assay kit, and then the OD value of each tube was read using a Synergy™ HT Multi-Mode Microplate Reader at a wavelength of 405 nm. All measurements were performed in triplicate.

2.4.3 RNA sequencing analysis

The transcriptome of the macrophytes from the MAB and nanobubble groups (at similar DO levels) was analysed after cultivation to obtain detailed expression profiles of genes involved in the response of the macrophytes to the growth conditions. The same amount tissues of three replications of each treatment were mixed together and used for

RNA-Seq experiments. The filtered differentially expressed genes (DEGs) were mapped to the GO database using GOseq[25] to obtain significantly enriched GO terms.

2.4.4 Plant hormones

To understand the regulatory effect of plant hormones on plant growth and development, accurate and efficient measurements of individual plant hormones in leaves and roots are required. HPLC-ESI-MS/MS was used for quantitation of endogenous plant hormones, which included 3-indoleacetic acid (IAA), salicylic acid (SA), jasmonic acid (JA) and jasmonic acid-isoleucine (JA-ILE). For each species of plant, 5 g plant tissue samples were taken randomly from leaves and roots and separated tissues were frozen with liquid nitrogen, then lyophilized tissue samples were ground to a powder by high-speed agitation with ceramic beads for 5 s. Metabolites were extracted from ground tissues using acetonitrile-water (1:1, v/v) and then centrifuged for 10 min at 12000 rpm at 4℃. A portion (2 μL) of sample was loaded onto a HPLC system (AcQuity UPLC, Waters, USA) equipped with a 50*2.1 mm Waters HSS T3 LC–MS column using a flow-rate of 2 μL /min and a binary solvent system comprising water with 0.1% (v/v) acetic acid (A) and acetonitrile with 0.1% (v/v) acetic acid (B) as mobile phases. The primary parameters of electrospray ionization mass spectrometry (Q exactive, Thermo, USA) were as follows: voltage: -2800V; temperature: 350°C; gas: nitrogen; nebulizing gas: 40 psi; auxiliary gas: 10 psi. All measurements were performed in triplicate.

2.5 Statistical analysis

The significance of differences in plant growth was analysed by one-way analysis of variance followed by Tukey's HSD test with $p < 0.05$. For RNA sequencing analysis, the read counts were adjusted with the edgeR program package using a one-scaling normalized

factor prior to differential gene expression analysis.[26] The p-value was adjusted using q-value, and the threshold for significantly different expression was set as "q-value<0.005 & |log2 (foldchange) |>1".[27] Origin 2018b (OriginLab, Northampton, MA, USA) was used for plotting.

3. Results and Discussion

3.1 Nanobubble generation and DO level in water

The mean particle sizes of the nanobubbles from the nanobubble aeration groups were similar and fell in to a range of 187.7-222.7 nm. The concentration of nanobubbles (<1000 nm) was 6.88×10^6 particles/mL in the L-NB group (Fig. 1a) and 1.23×10^7 particles/mL in the M-NB group (Fig. 1b). Higher nanobubble concentrations were observed in the H-NB and S-NB groups with 3.45×10^7 and 2.70×10^8 particles/mL, respectively (Fig. 1c and d). Notably, the control and macrobubble groups consistently contained $<10^5$ particles/mL nanobubbles (data not shown). In the practical application, high concentrations of nanobubble (up to 10^8 particles/mL) could be formed in the water close to the nanobubble pump during the eutrophication remediation. However, the concentrations would be decreased along with the increased distance from the pump due to the dilution effect and nanobubble consumptions, e.g. oxidation with organic pollutants. Therefore, the whole range of the nanobubble concentrations, ranging from 10^5 particles/mL (the background concentration) to 10^8 particles/mL, was conducted in this study to investigate the effect of the nanobubble on the aquatic plant growth.

Fig. S1 showed the difference of the DO levels in all groups, which was positively affected by the timing of nanobubble generation[21]. However, under current operations in this study, the DO levels in all groups fell into a relatively small range of 7.08-7.65 and 7.01-7.26

mg/L in *Iris* and *Echinodorus* cultures, respectively (Table 2). For both plants, similar DO levels were observed in control, L-NB and M-NB groups, with statistically lower values than those in other groups. The fluctuation of DO levels during the experiment was relatively greater in the emergent *Iris* groups than the submergent *Echinodorus* groups (Fig. S1). In addition, no significant difference in pH levels was observed among all *Iris* groups. However, pH level increased slightly along with increased nanobubble concentration in the groups cultivated with *Echinodorus* (Fig. S2). Specifically, the average pH increased from 8.41 ± 0.14 in the control group to 8.68 ± 0.08 in the S-NB group, which may be induced by the positive growth response of the *Echinodorus* to the NB aeration (Fig. S2).

During aeration, the bubble size distribution affects the DO content in water, because bubbles of a smaller size have a proportionally greater surface area than large bubbles and can give a better oxygen transfer rate. However, perhaps controversially, in the current investigation nano-scale bubble aeration did not result in a very high DO level in water. Previous studies have observed that nanobubbles are stable for days.[28,29] Atomic force microscopy (AFM) has detected heterogeneous pressures inside nanobubbles, which was modelled in a molecular dynamics simulation as a high-gas-density state.[30] The oxygen inside nanobubbles may exist as an aggregation rather than the ideal gas phase of dissolved oxygen, and the diffusion of the oxygen inside nanobubbles is likely to be slow and to take place over a long period of time. Thus, traditional instantaneous measurements of the DO level of water samples can only detect the dissolved phase of oxygen, but not fully reflect the total contribution of nanobubbles to any increase in gas transfer.

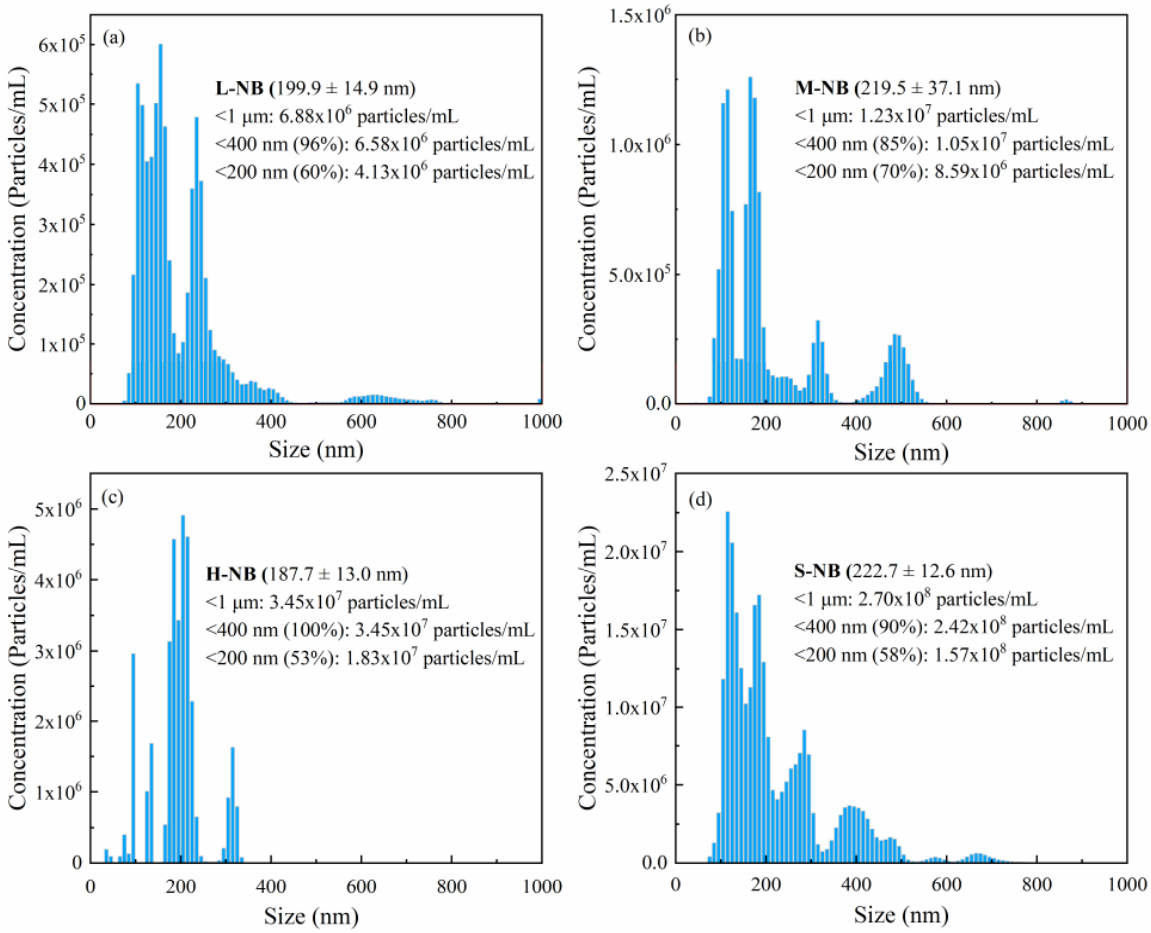

Figure 1. Nanobubble size distribution in L-NB (a), M-NB (b), H-NB (c) and S-NB (d) groups. L-NB, M-NB, H-MB, S-NB represent low, medium, high and super-high nanobubble concentration groups, respectively.

Table 2

The average DO levels in water during the cultivation of both aquatic plant species.

	Dissolved oxygen (mg/L)					
	Control	**MAB**	**L-NB**	**M-NB**	**H-NB**	**S-NB**
Iris	7.08 ± 0.50^{b}	7.49 ± 0.56^{ab}	7.13 ± 0.45^{b}	7.29 ± 0.47^{ab}	7.52 ± 0.65^{ab}	7.65 ± 0.61^{a}
Echinodorus	7.01 ± 0.25^{b}	7.21 ± 0.19^{ab}	7.02 ± 0.30^{b}	7.08 ± 0.27^{ab}	7.26 ± 0.18^{a}	7.23 ± 0.19^{ab}

MAB, L-NB, M-NB, H-MB, S-NB represent macrobubble aeration, low, medium, high and super-high nanobubble concentration groups, respectively. Error bars indicate standard

deviations. The superscript letters indicate significant differences ($p < 0.05$) compared with other groups of the same plant.

3.2 Plant morphology response to nanobubbles

For *Iris*, the transplant-survival rates were 68.8%, 81.3% 81.3%, 93.8%, 100% and 100% for the control, MAB, L-NB, M-NB, H-NB and S-NB groups, respectively. The biomass growth ratios were higher in all nanobubble treatment groups (1.39 ± 0.15 - 1.54 ± 0.08), followed by the macrobubble-aerated group (1.32 ± 0.14) and the control group (1.28 ± 0.09) (Fig. 2a). In the nanobubble aeration groups, the plant biomass growth ratio increased along with increasing nanobubble concentration and reached the highest value of 1.54 ± 0.08 in the H-NB group (nanobubble concentration of 3.45×10^7 particles/mL). However, after further increasing of the nanobubble concentration (2.70 × 108 particles/mL) in the S-NB group, the biomass growth ratio reduced to 1.41 ± 0.14, the significant difference were observed between H-NB and S-NB groups (Figure 2a, $p<0.05$). In summary, the plant biomass growth ratios in the MAB, L-NB, M-NB, H-NB and S-NB groups were 3%, 8%, 14%, 20% and 9.5% higher than that in the control group, respectively. The length of the *Iris* root followed a similar trend with average root lengths of 12.04 ± 2.24, 13.78 ± 2.51, 14.29 ± 2.71 and 14.31 ± 2.09 cm in the L-NB, M-NB, H-NB and S-NB groups (Fig. 2b and Fig. S3), compared with the macrobubble-aerated group (10.59 ± 2.26 cm) and the control group (10.44 ± 3.12 cm). No significant difference in leaf length or chlorophyll content between the various groups of *Iris* was observed, which may be due to the emergent plant leaf being out of the water and therefore less likely to be influenced by the nanobubbles in the water. The growth of the root, which is in direct contact with the nanobubbles, may be promoted by the increased aerobic respiration of the plant, which could cause new root formation.[31–33]

Regarding the submergent species, *Echinodorus*, the transplant survival rate was 100%. The biomass growth ratios (around 1.5) in all macrobubble- and nanobubble-aerated groups were not significantly different (Fig. 2c). However, these values were generally significantly higher than that of the control group (1.24 ± 0.14). The length of both root and leaf in these groups followed the same trend. Although a similar biomass increase was observed in all aerated groups, some degradation of chlorophyll content and yellowing occurred in nanobubble-aerated groups (Fig. 2d), which is consistent with our previous study[22]. The threshold nanobubble concentration required to affect the chlorophyll content was identified in the M-NB group (1.51 mg/g FW). The excess nanobubbles present in the H-NB (3.45×10^7 particles/mL) and S-NB (2.70×10^8 particles/mL) groups drove the chlorophyll content significantly lower (1.29 and 0.72 mg/g FW, respectively), supporting the notion that photosynthesis is likely to be adversely affected by high concentrations of nanobubbles.

The submergent and emergent plants exhibited a different response to nanobubbles, with the emergent species seeming to have a higher tolerance, which may be due to the different spatial locations of plant parts and/or species-specific antioxidant capacity.[22] Nevertheless, it can be concluded that aquatic plant growth can benefit from exposure to certain concentrations of nanobubbles, but overdosing with nanobubbles can damage plant growth (biomass) and health (chlorophyll content).

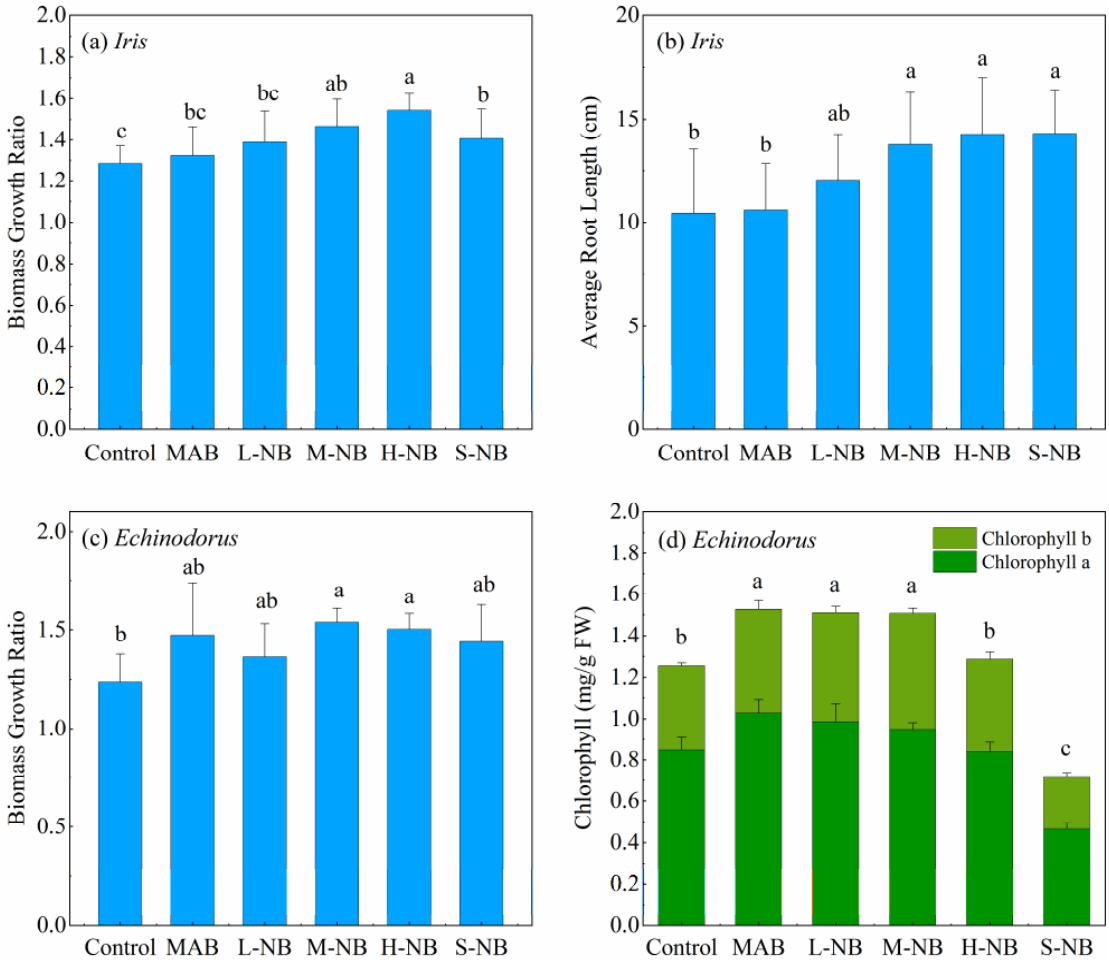

Figure 2. Biomass growth ratio of *Iris* (a) and *Echinodorus* (c), average root length of *Iris* (b), and chlorophyll content of *Echinodorus* (c) at the end of the experiment. MAB, L-NB, M-NB, H-MB, S-NB represent macrobubble aeration, low, medium, high and super-high nanobubble concentration groups, respectively. Error bars indicate standard deviations. The different letters indicate significant differences ($p < 0.05$) compared with other groups of the same plant.

3.3 Effect of nanobubbles on plant physiology

3.3.1 Reactive oxygen species (ROS) and total antioxidant capacity (T-AOC)

Besides changes in morphology, plants can also modify their physiology in response to differences in environmental conditions, including in temperature, light and growth media. A growth medium with a high level of DO[34] and/or oxidising substances[16,17] is likely to

stimulate endogenous ROS generation within plant tissues and thus to promote plant growth.[18] Accordingly, in the current investigation the concentrations of ROS (superoxide radical ($^{\bullet}O_2^-$)) in *Iris* were significantly higher in MAB and nanobubble treatment groups (6.12-7.49 and 2.35-6.33 μg/g FW in the leaf and root, respectively) compared with that (4.87 and 1.79 μg/g FW in the leaf and root, respectively) in the control group (Fig. 3a), with the only exception being the S-NB group (3.55 μg/g FW in the leaf). Notably, the highest ROS levels appeared in the H-NB group and then decreased at the higher nanobubble concentration in the S-NB group. This may be due to the increased levels of ROS accumulating within plants, which thereby induce oxidative stress. This is in line with the biomass results (Fig. 2a), where the highest *Iris* biomass was found in the H-NB group. In response to extremely oxidising conditions, the plant oxidative stress response will be stimulated, leading to an increase in total antioxidant capacity (T-AOC), which will act to maintain ROS at an appropriate level.[19] In root, the T-AOC increased consistently with nanobubble concentration from 9.79 U/g FW in the control group to around 26 U/g FW (MAB, L-NB and M-NB groups) and 50.79 U/g FW in the H-NB group, and reached the highest level (84.96 U/g FW) in the S-NB group (Fig. 3b). In the leaf, T-AOC content showed a similar trend and increased from approximately 170 U/g FW to 230 U/g FW. The increase in ROS scavengers under highly oxidizing conditions[18] may explain the significantly lower ROS concentration in the S-NB plants compared to the H-NB group (Fig. 3a).

Echinodorus is expected to behave differently to the emergent species, *Iris*, because the whole plant grows under the water and thus has direct contact with nanobubbles. Because there was insufficient *Echinodorus* root for measurements, ROS and T-AOC contents were only tested in leaves. The superoxide radical ($^{\bullet}O_2^-$) content in the leaf, compared to the control

(23.76 μg/g FW), increased in the macrobubble-aerated group (27.28 μg/g FW), and increased with nanobubble concentration in the L-NB (27.32 μg/g FW) and M-NB (32.42 μg/g FW) groups. However, the content then decreased to 28.73 μg/g FW and 22.95 μg/g FW in the H-NB and S-NB groups, respectively (Fig. 3c). The same trend was also observed for T-AOC content in the leaves, but with the highest value (125.51 U/g FW) in the H-NB group, decreasing to 105.23 U/g FW in S-NB plants (Fig. 3d).

Thus, because DO levels were similar in the MAB and nanobubble groups, the above effect on plant oxidant and antioxidant levels is probably due to the presence of nanobubbles. A previous study reported a consistent increase in antioxidant enzyme activity in soybean after 48 h exposure to increased oxidative stress,[35] consistent with our present findings. While oxygen promotes plant growth, this may become hyperoxia stress when the concentration of nanobubbles in the water exceeds 3.45×10^7 and 1.23×10^7 particles/mL for *Iris* and *Echinodorus*, respectively. It is worth noting that the thresholds for other plants may be different due to species-specific antioxidant capacities for each plant.[22]

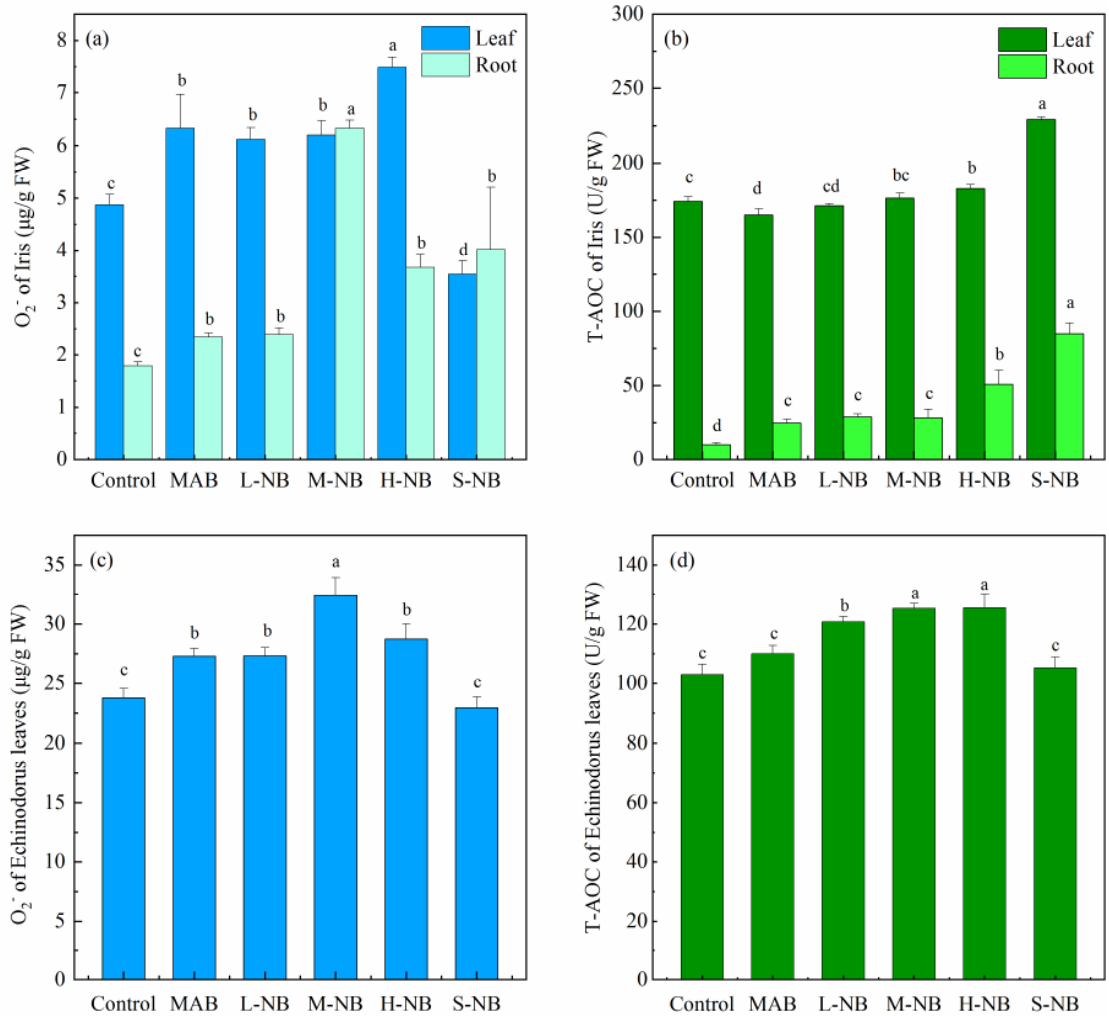

Figure 3. Superoxide radical concentration (a) and total antioxidant capacity (T-AOC) (b) in the leaf and root of *Iris*; superoxide radical concentration (c) and T-AOC (d) in the leaf of *Echinodorus* at the end of the experiment. MAB, L-NB, M-NB, H-MB and S-NB represent macrobubble aeration, low, medium, high and super-high nanobubble concentration groups, respectively. Error bars indicate standard deviations. The different letters indicate significant differences ($p < 0.05$) compared with other groups of the same plant.

3.3.2 Transcriptional response

Based on the effects on plant morphology, *Iris* from the MAB and H-NB groups, and *Echinodorus* from the MAB and S-NB groups, were selected to identify differentially expressed genes (DEGs) that respond to nanobubble and macrobubble treatment at similar

DO levels. In total, 1321 upregulated and 1074 downregulated unigenes were identified from *Iris* in the H-NB group, compared to MAB plants (Fig. 4a). The molecular functions of these genes are indicated by the associated GO terms, and several that were significantly enriched in *Iris* plants relate to oxygen binding, transfer and reduction (Fig. 4b). Plants use hemoglobins to bind and transfer oxygen efficiently,[36] which is then used for respiration. The upregulation of genes related to "heme binding", "tetrapyrrole binding" and "iron ion binding" points to an enhanced ability to use oxygen in nanobubble-treated plants. In addition, the term "oxidoreductase activity, acting on paired donors, with incorporation or reduction of molecular oxygen" was also enriched, which indicates that the plants have received excessive molecular oxygen, leading to the genes involved in the reduction of molecular oxygen being overrepresented. The enhancement of oxygen delivery to plants induces ROS production (Fig. 3a), consistent with a group of 141 genes under the "oxidation-reduction process" umbrella being the most dominant group in the biological processes category; of these, 103 were upregulated unigenes and 38 were downregulated (Fig. 4b, Table S1). In addition, most genes related to "defense response" and "response to stress" in the biological process category were also upregulated, implying that the nanobubbles induce hyperoxia stress (Fig. 4b).

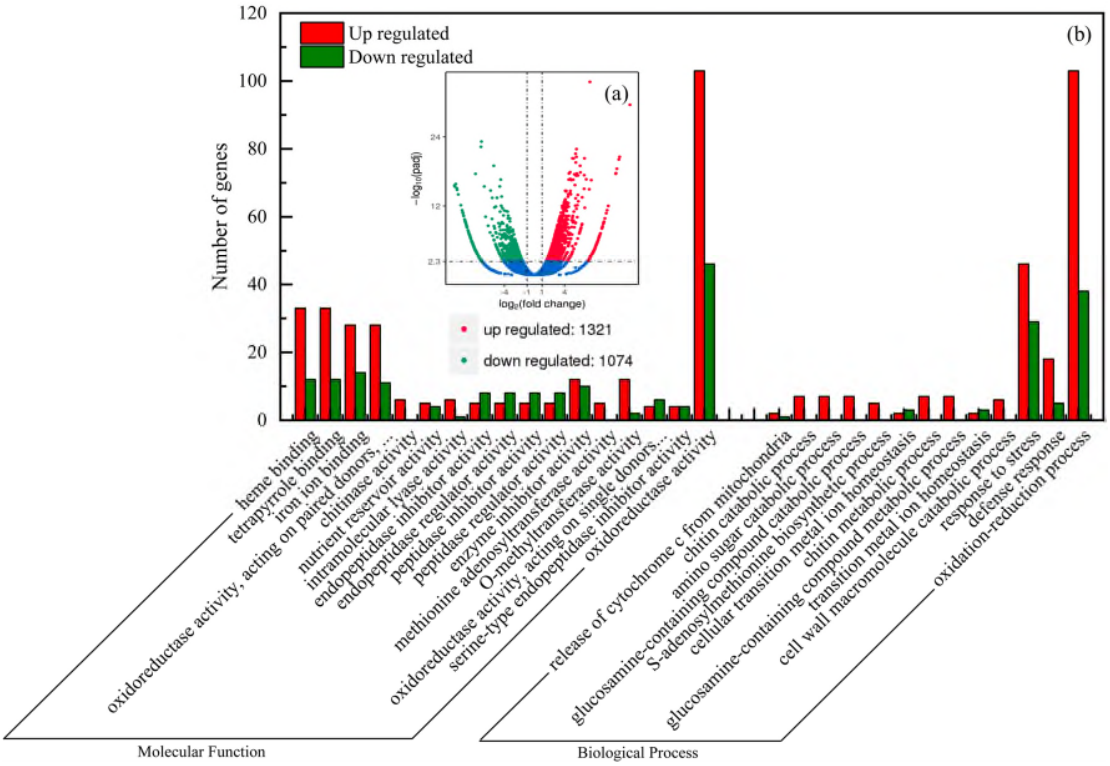

Figure 4. (a) Gene expression changes in *Iris* plants of the H-NB group (DO = 7.52 ± 0.65 mg/L) compared with the MAB group (DO = 7.49 ± 0.56 mg/L). (b) Significantly enriched Gene Ontology (GO) classification of differentially expressed genes (p<0.05).

In *Echinodorus*, there were significantly more downregulated (4209) than upregulated (2140) genes in plants from the S-NB group compared to the MAB group (Fig. 5a). The submergent nature of *Echinodorus*, meaning that it was completely immersed in the bulk nanobubble water, may lead to more oxygen stress than in *Iris* and the subsequent breakdown of the antioxidant system. Thus, 131 upregulated unigenes and 359 downregulated unigenes were found under the 'oxidation-reduction process' heading (Table S2). In addition, most genes related to photosynthesis, such as 'thylakoid', 'thylakoid membrane', 'photosystem' and 'photosynthetic membrane', were downregulated (Fig. 5b). The chloroplast structure was severely damaged and chlorophyll content significantly decreased at high nanobubble concentrations (Fig. 2d and Fig. 5b), which is also consistent with hyperoxia stress. It has

been documented that the rate of photosynthesis can be inhibited by high oxygen concentrations.[37–39] Oxygen is a competitive inhibitor of carbon dioxide fixation and can result in a significant decrease (up to 60%) in photosynthetic efficiency and photosynthetic output.[40] Therefore, genes with the 'metabolic process' term were downregulated, in accordance with a reduction in plant physiological activity. In our previous experiments, the growth of *Echinodorus* was significantly inhibited (25%) after 60 days cultivation at a high nanobubble concentration.[22]

In summary, RNA sequencing analysis shows that the ability to bind, transfer and reduce oxygen and the stress resistance capacity in *Iris* were enhanced by nanobubble treatment compared with macrobubble treatment at a similar DO level. However, the antioxidant system of *Echinodorus* collapsed and both photosynthesis and general metabolic processes were inhibited.

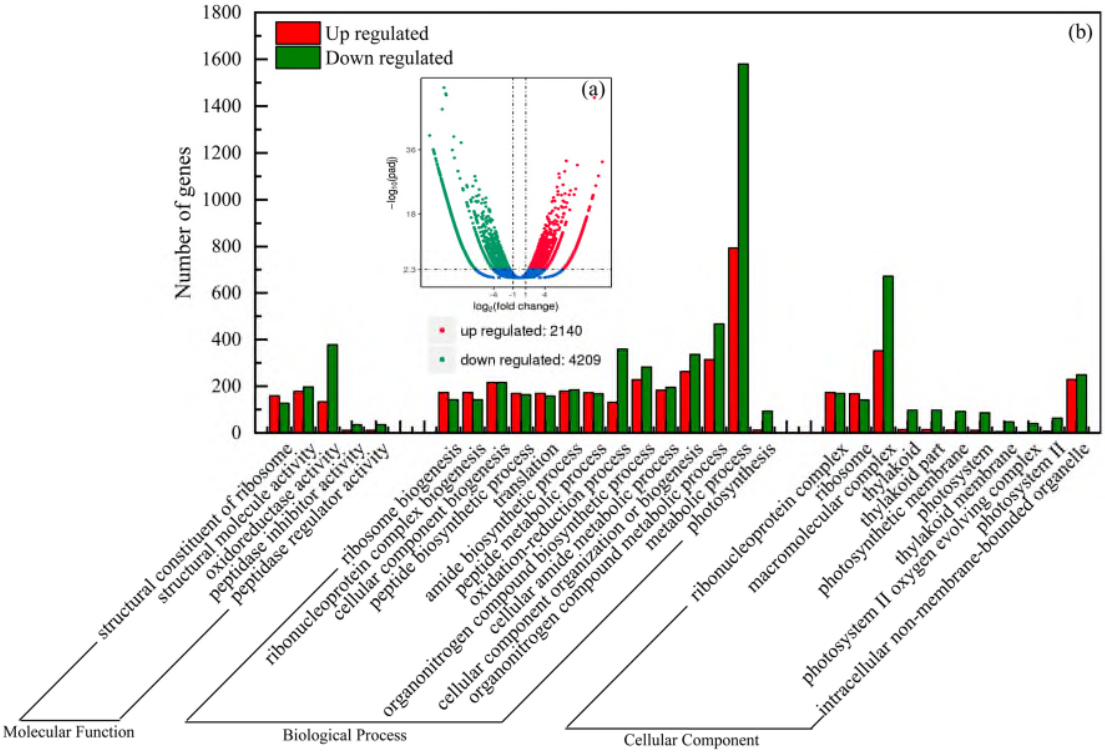

Figure 5. (a) Gene expression changes of *Echinodorus* in the S-NB group (DO = 7.23 ± 0.19 mg/L) compared with the MAB group (DO = 7.21 ± 0.19 mg/L). (b) Significantly enriched Gene Ontology (GO) classification of differentially expressed genes (p<0.05).

3.3.3 Plant hormone generation

Diverse aspects of plant growth and development are controlled by the plant hormone network, which allows plants to adapt and survive in highly dynamic natural environments, including the change of the oxygen level.[41] At similar DO levels in the MAB and nanobubble groups, the 3-indoleacetic acid (IAA) contents in both plant species were significantly higher in nanobubble treatment groups (M-NB, H-NB and S-NB) than in the MAB group. Moreover, the IAA content increased with increasing nanobubble concentration from 31.25 ng/g (MAB group) to 84.63 ng/g (S-NB group) for *Iris*, and 1.04 ng/g (MAB group) to 1.55 ng/g (S-NB group) for *Echinodorus* (Table 3). IAA can promote root initiation and induces both growth of pre-existing roots and adventitious root formation.[42] Therefore, the alteration in the plant root architecture was probably achieved largely through the high levels of IAA (Fig. 2b, Fig. S3),[43] which thereby promoted an increase in biomass (Fig. 2a). In addition, the chlorophyll degradation (photosynthesis damage) we observed may also be related to the increased IAA levels in *Echinodorus* (Fig. 2d and Fig. 5b). This is supported by a previous study, which showed that the chloroplast membrane system was less developed and the chlorophyll content was lower in wheat coleoptiles treated with IAA.[44] Endogenous ROS generation in plants mainly results from side-reactions of the photosynthesis process,[45] and therefore IAA is likely to reduce ROS generation in the S-NB group by remodelling the photosynthetic apparatus and thereby minimizing oxidative damage (Fig. 2d and Fig. 5).[41]

Moreover, the levels of salicylic acid (SA), jasmonic acid (JA) and jasmonic acid-isoleucine (JA-ILE), which play important roles in plant responses to a wide range of biotic

and abiotic stresses,[46] also significantly increased in the nanobubble groups (Table 3). SA content reached the highest levels in the S-NB group in both plant species, while JA and JA-ILE content first increased with increasing nanobubble concentration, and then decreased in the S-NB group. These elevated hormone levels further demonstrate that nanobubbles cause hyperoxia stress in plants, which trigger plant defences and promote physiological adaptation.

The results described so far indicate that exposure to nanobubbles can alter redox homeostasis, gene expression and hormone generation in plants. Previous studies show that the ROS signalling pathway consists of an elaborate network that exhibits frequent crosstalk with gene[47] and hormone[41] pathways. The endogenous ROS induced by nanobubbles can thus regulate the growth and development of plants in concert with T-AOC, genes and plant hormones.

Table 3

Hormone changes in plants of different groups with similar DO levels.

		Phytohormone (ng/g)			
		IAA	**SA**	**JA**	**JA-ILE**
Iris root	MAB	31.25 ± 2.40^{d}	55.21 ± 2.74^{b}	1.73 ± 0.08^{d}	1.40 ± 0.05^{c}
	M-NB	44.73 ± 1.90^{c}	58.37 ± 3.87^{b}	6.35 ± 0.35^{b}	2.06 ± 0.21^{b}
	H-NB	56.18 ± 2.47^{b}	52.47 ± 4.47^{b}	8.44 ± 0.42^{a}	3.41 ± 0.34^{a}
	S-NB	84.63 ± 2.64^{a}	87.34 ± 2.56^{a}	3.90 ± 0.12^{c}	3.15 ± 0.31^{a}
Echinodorus leaf	MAB	1.04 ± 0.08^{c}	/	5.10 ± 0.39^{c}	2.54 ± 0.26^{a}
	M-NB	1.12 ± 0.15^{c}	/	9.90 ± 2.89^{b}	3.01 ± 0.62^{a}
	H-NB	1.39 ± 0.02^{b}	2.96 ± 0.09^{b}	16.61 ± 1.14^{a}	2.39 ± 0.16^{a}
	S-NB	1.55 ± 0.04^{a}	3.50 ± 0.17^{a}	2.43 ± 0.31^{d}	0.98 ± 0.28^{b}

IAA, SA, JA, JA-ILE represent 3-indoleacetic acid, salicylic acid, jasmonic acid, jasmonic acid-isoleucine, respectively. Error bars indicate standard deviations. The different letters indicate significant differences ($p < 0.05$) compared with other groups of the same plant.

3.4 Overall mechanisms

The principal component analysis (PCA) was used to visualise the effect of nanobubble concentrations on plant growth responses (Fig. 6a and b). The growth medium conditions

(DO and nanobubble concentrations), plant morphology parameters (biomass growth ratio and root length for *Iris*, biomass growth ratio and chlorophyll content for *Echinodorus*), and plant physiology parameters (ROS and T-AOC for *Iris* leaf and root, and for *Echinodorus* leaf) were included in the analysis.

For both species (Fig. 6a and b), the factor of nanobubble concentration clearly drives the S-NB groups away from other groups in the coordinate. Closer examination of the *Echinodorus* data (Fig. 6b) shows that the H-NB groups also follow the direction of the nanobubble concentration factor, causing them to differentiate from other groups. This agrees with our results showing that the nanobubble concentration thresholds that significantly influence the growth of *Iris* and *Echinodorus* are likely 3.45×10^7 particles/mL (H-NB group) and 1.23×10^7 particles/mL (M-NB group), respectively: below the threshold, increasing nanobubble concentration can significantly improve plant growth (Fig. 2). The patterns of other groups cluster together in a right-up direction for both species (Fig. 6) as the nanobubble concentration increases (from control to MAB and to H-NB groups). Biomass growth ratio, ROS (for *Iris* root or *Echinodorus* leaf), root length (*Iris*) and chlorophyll content (*Echinodorus*) are the main factors contributing to the right-up direction. Endogenous ROS appears to be a major factor affecting plant biomass (Fig. 6), which is consistent with the improvement in plant performance that can occur with appropriate levels of ROS. In addition, the increase in nanobubble concentration contributed to the T-AOC content increase in *Iris* leaf and root (Fig. 6a), but chlorophyll content changed in the opposite direction, i.e. decreased, with nanobubble concentration in *Echinodorus* (Fig. 6b).

The emergent species clearly has a higher tolerance of nanobubbles. Below the threshold, The enhanced oxygen delivery in water resulting from the stability and high gas

density of nanobubbles[48,49] may promote plant aerobic respiration and the generation of endogenous ROS in plants, resulting in the increase of antioxidant capacity in plants and superior plant growth. However, when the nanobubble concentration exceeds the threshold, the toxicity of oxygen will become dominant and induce hyperoxia stress, particularly in submergent plants, which may result in collapse of the antioxidant system and the inhibition of photosynthesis. The physiological responses of the aquatic plants may also be caused by the oxidation substances, such as the free radicals released from the nanobubble. Further studies are needed to investigate the free radicals and their interactions with the relevant hyperopia stress of aquatic plants.

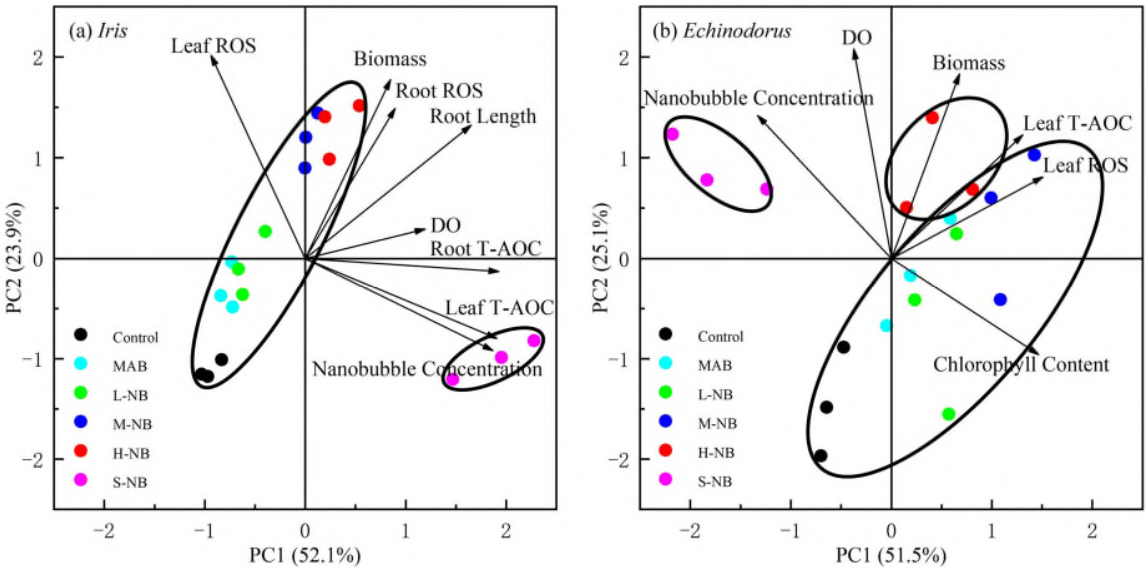

Figure 6. Principal component analysis (PCA) of results from the morphological and physiological responses of *Iris* (a) and *Echinodorus* (b) in the various groups. The points from different experimental groups in the same circle represent their clear differences with the data points in other circles during the PCA analysis.

Bulk nanobubble and interfacial nanobubble technology have both been used for the restoration of eutrophic and black-odour water in recent years. As a sustainable and efficient technology, nanobubble technology offers many advantages with respect to internal nutrient

loading control, HAB removal and water quality improvement. Generally, using a higher concentration of nanobubbles or pure oxygen nanobubbles results in a greater improvement in water quality. However, natural water restoration is a systematic process, of which the restoration of aquatic vegetation following an improvement in the water quality is an important part. Our results demonstrate that nanobubbles can promote plant aerobic respiration and the generation of endogenous ROS in plants, which improve plant growth. The energy consumption (31.25 W/m^3) in the M-NB group was one fifth of that (150 W/m^3) in the MAB group (Table 1), but exhibited a better performance in promoting plant growth. Nevertheless, extremely high nanobubble concentrations induce hyperoxia stress and inhibit plant physiological activity, such as oxidation-reduction, photosynthesis and metabolic processes. Notably, the identified thresholds for the aquatic plants were confirmed under experimental conditions with the homogenised nanobubble concentration. The nanobubble concentrations would vary in different areas of the natural waters, which need to be considered when using the current finding to guide the practical application.

4. Conclusion

This study investigated the morphological and physiological response of both emergent (*Iris*) and submergent (*Echinodorus*) aquatic plants during the later stage of the nanobubble-induced water restoration process. This study demonstrated the nanobubble concentration thresholds for the switch from growth promotion to growth inhibition are 3.45×10^7 and 1.23×10^7 particles/mL for *Iris* and *Echinodorus*, respectively. The growth of both aquatic plants was promoted, under this threshold, due to the improved aerobic respiration and the generation of ROS in plants. However, excessed nanobubbles could induce hyperoxia stress, affect the expression of genes and the generation of relevant hormones. Therefore, using a

higher concentration of nanobubbles could achieve the effective water quality improvement, however, appropriate concentrations of nanobubble (approximate 10^7 particles/mL) should be controlled to facilitate the aquatic vegetation growth towards throughout eutrophication management and water restoration. Meanwhile, the potentially different thresholds for other aquatic vegetation species should be further studied.

ASSOCIATED CONTENT

The Supporting Information is available free of charge at http://pubs.acs.org.

Notes

The authors declare no competing financial interest.

Acknowledgements

This work was supported in part by The National Major Science and Technology Project of China (2017ZX07201002) and partially by a scholarship from the China Scholarship Council (CSC).

Reference

(1) Agarwal, A.; Ng, W. J.; Liu, Y. Principle and Applications of Microbubble and Nanobubble Technology for Water Treatment. *Chemosphere* **2011**, *84* (9), 1175–1180.

(2) Takahashi, M.; Chiba, K.; Li, P. Free-Radical Generation from Collapsing Microbubbles in the Absence of a Dynamic Stimulus. *J. Phys. Chem. B* **2007**, *111* (6), 1343–1347.

(3) Li, P.; Song, Y.; Yu, S. Removal of Microcystis Aeruginosa Using Hydrodynamic Cavitation: Performance and Mechanisms. *Water Res.* **2014**, *62*, 241–248.

(4) Sun, Y.; Wang, S.; Niu, J. Microbial Community Evolution of Black and Stinking Rivers during in Situ Remediation through Micro-Nano Bubble and Submerged Resin Floating Bed Technology. *Bioresour. Technol.* **2018**, *258*, 187–194.

(5) Wu, Y.; Lin, H.; Yin, W.; Shao, S.; Lv, S.; Hu, Y. Water Quality and Microbial Community Changes in an Urban River after Micro-Nano Bubble Technology in Situ Treatment. *Water* **2019**, *11* (1), 66.

(6) Zhang, H. Combating Hypoxia/Anoxia at Sediment-Water Interfaces: A Preliminary Study of Oxygen Nanobubble Modified Clay Materials. *Sci. Total Environ.* **2018**, 11.

(7) Shi, W.; Pan, G.; Chen, Q.; Song, L.; Zhu, L.; Ji, X. Hypoxia Remediation and Methane Emission Manipulation Using Surface Oxygen Nanobubbles. *Environ. Sci. Technol.* **2018**, *52* (15), 8712–8717.

(8) SOLitude. Oxygenate Your Waterbody With Nanobubble Aeration https://www.solitudelakemanagement.com/ultra-fine-nanobubble-technology. **2019**, (accessed Jun 16, 2020).

(9) Gunther, T. Lakes can breathe again: Introducing pure oxygen nanobubble solution https://smartwatermagazine.com/news/lg-sonic/lakes-can-breathe-again-introducing-pure-oxygen-nanobubble-solution. **2019**, (accessed Jun 16, 2020).

(10) Zhang, Y.; Jeppesen, E.; Liu, X.; Qin, B.; Shi, K.; Zhou, Y.; Thomaz, S. M.; Deng, J. Global Loss of Aquatic Vegetation in Lakes. *Earth-Sci. Rev.* **2017**, *173*, 259–265.

(11) Dat, J. F.; Folzer, H.; Parent, C.; Badot, P.-M.; Capelli, N. Hypoxia Stress: Current Understanding and Perspectives. Floriculture, Ornamental and Plant Biotechnology: Advances and Topical Issues 3. **2006**, 664-674.

(12) Ahmed, A.; Shi, X.; Hua, L.; Manzueta, L.; Qing, W.; Marhaba, T.; Zhang, W. Influences of Air, Oxygen, Nitrogen, and Carbon Dioxide Nanobubbles on Seed Germination and Plant Growth. *J. Agric. Food Chem.* **2018**, *66*.

(13) Park, J.-S.; Kurata, K. Application of Microbubbles to Hydroponics Solution Promotes Lettuce Growth. *HortTechnology* **2009**, 212–215.

(14) Ikeura, H.; Tsukada, K.; Tamaki, M. Effect of Microbubbles in Deep Flow Hydroponic Culture on Spinach Growth. *J. Plant Nutr.* **2017**, *40* (16), 2358–2364.

(15) Wu, Y.; Lyu, T.; Yue, B.; Tonoli, E.; Verderio, E. A. M.; Ma, Y.; Pan, G. Enhancement of Tomato Plant Growth and Productivity in Organic Farming by Agri-Nanotechnology Using Nanobubble Oxygation. *J. Agric. Food Chem.* **2019**, *67* (39), 10823–10831.

(16) Liu, S.; Oshita, S.; Kawabata, S.; Makino, Y.; Yoshimoto, T. Identification of ROS Produced by Nanobubbles and Their Positive and Negative Effects on Vegetable Seed Germination. *Langmuir* **2016**, *32* (43), 11295–11302.

(17) Liu, S.; Oshita, S.; Makino, Y.; Wang, Q.; Kawagoe, Y.; Uchida, T. Oxidative Capacity of Nanobubbles and Its Effect on Seed Germination. *ACS Sustain. Chem. Eng.* **2016**, *4* (3), 1347–1353.

(18) Mittler, R. ROS Are Good. *Trends Plant Sci.* **2017**, *22* (1), 11–19.

(19) Morimoto, H.; Iwata, K.; Ogonuki, N.; Inoue, K.; Atsuo, O.; Kanatsu-Shinohara, M.; Morimoto, T.; Yabe-Nishimura, C.; Shinohara, T. ROS Are Required for Mouse Spermatogonial Stem Cell Self-Renewal. *Cell Stem Cell.* **2013**, *12* (6), 774–786.

(20) Ikeura, H.; Takahashi, H.; Kobayashi, F.; Sato, M.; Tamaki, M. Effect of Different Microbubble Generation Methods on Growth of Japanese Mustard Spinach. *J. Plant Nutr.* **2017**, *40* (1), 115–127.

(21) Ikeura, H.; Takahashi, H.; Kobayashi, F.; Sato, M.; Tamaki, M. Effects of Microbubble Generation Methods and Dissolved Oxygen Concentrations on Growth of Japanese Mustard Spinach in Hydroponic Culture. *J. Hortic. Sci. Biotechnol.* **2018**, *93* (5), 483–490.

(22) Wang, S.; Liu, Y.; Li, P.; Wang, Y.; Yang, J.; Zhang, W. Micro-Nanobubble Aeration Promotes Senescence of Submerged Macrophytes with Low Total Antioxidant Capacity in Urban Landscape Water. *Environ. Sci. Water Res. Technol.* **2020**, *6* (3), 523–531.

(23) Das, K.; Samanta, L.; Chainy, G. B. N. A Modified Spectrophotometric Assay of Superoxide Dismutase Using Nitrite Formation by Superoxide Radicals. *IJBB Vol373.* **2000**, 6.

(24) Schneider, K.; Schlegel, H. G. Production of Superoxide Radicals by Soluble Hydrogenase from Alcaligenes Eutrophus H16. *Biochem. J.* **1981**, *193* (1), 99–107.

(25) Young, M. D.; Wakefield, M. J.; Smyth, G. K.; Oshlack, A. Gene Ontology Analysis for RNA-Seq: Accounting for Selection Bias. *Genome Biol.* **2010**, *11* (2), R14.

(26) Robinson, M. D.; McCarthy, D. J.; Smyth, G. K. EdgeR: A Bioconductor Package for Differential Expression Analysis of Digital Gene Expression Data. *Bioinformatics.* **2010**, *26* (1), 139–140.

(27) Storey, J. D.; Tibshirani, R. Statistical Significance for Genomewide Studies. *Proc. Natl. Acad. Sci. U. S. A.* **2003**, *100* (16), 9440–9445.

(28) Tan, B. H.; An, H.; Ohl, C.-D. How Bulk Nanobubbles Might Survive. *Phys. Rev. Lett.* **2020**, *124* (13), 134503.

(29) Chen, C.; Li, J.; Zhang, X. The Existence and Stability of Bulk Nanobubbles: A Long-Standing Dispute on the Experimentally Observed Mesoscopic Inhomogeneities in Aqueous Solutions. *Commun. Theor. Phys.* **2020**, *72* (3), 037601.

(30) Zhang, X. H.; Maeda, N.; Craig, V. S. J. Physical Properties of Nanobubbles on Hydrophobic Surfaces in Water and Aqueous Solutions. *Langmuir* **2006**, *22* (11), 5025–5035.

(31) Soffer, H.; Burger, D. W. Effects of Dissolved Oxygen Concentrations in Aero-Hydroponics on the Formation and Growth of Adventitious Roots. **1998,** 5.

(32) Suyantohadi, A.; Kyoren, T.; Hariadi, M.; Purnomo, M. H.; Morimoto, T. Effect of High Consentrated Dissolved Oxygen on the Plant Growth in a Deep Hydroponic Culture under a Low Temperature. *IFAC Proc. Vol.* **2010**, *43* (26), 251–255.

(33) Kurashina, Y.; Yamashita, T.; Kurabayashi, S.; Takemura, K.; Ando, K. Growth Control of Leaf Lettuce with Exposure to Underwater Ultrasound and Dissolved Oxygen Supersaturation. *Ultrason. Sonochem.* **2019**, *51*, 292–297.

(34) Bartosz, G. Oxidative stress in plants. Acta Physiol Plant. **1997**, 19, 47–64.

(35) Simontacchi, M.; Caro, A.; Puntarulo, S. Oxygen-Dependent Increase of Antioxidants in Soybean Embryonic Axes. *Int. J. Biochem. Cell Biol.* **1995**, *27* (11), 1221–1229.

(36) Hardison, R. C. A Brief History of Hemoglobins: Plant, Animal, Protist, and Bacteria. *Proc. Natl. Acad. Sci. U. S. A.* **1996**, *93* (12), 5675–5679.

(37) Wroblewska, B.; Mostowska, A.; Poskuta, J. The Effect of Oxygen Concentration on Chloroplast Development, Chlorophyll Synthesis and Starch Accumulation in Etiolated Bean Seedlings upon Illumination. *Environ. Exp. Bot.* **1994**, *34* (2), 153–163.

(38) Turner, J. S.; Brittain, E. G. Oxygen as a Factor in Photosynthesis. *Biol. Rev.* **1962**, *37* (1), 130–170.

(39) Zelitch, I. *Photosynthesis, Photorespiration, And Plant Productivity*; Elsevier Science, 2012.

(40) Mohr, H.; Schopfer, P. *Plant Physiology*; Springer Science & Business Media, **1995**.

(41) Tognetti, V. B.; Mühlenbock, P.; Breusegem, F. V. Stress Homeostasis – the Redox and Auxin Perspective. *Plant Cell Environ.* **2012**, *35* (2), 321–333.

(42) Walker, P. M. B. *Chambers Dictionary of Science and Technology*; London : Chambers, **1999**.

(43) Pandey, V.; Bhatt, I. D.; Nandi, S. K. Chapter 20 - Role and Regulation of Auxin Signaling in Abiotic Stress Tolerance. In *Plant Signaling Molecules*; Khan, M. I. R., Reddy, P. S., Ferrante, A., Khan, N. A., Eds.; Woodhead Publishing, **2019**; pp 319–331.

(44) Volfová, A.; Chvojka, L.; Friedrich, A. The Effect of Kinetin and Auxin on the Chloroplast Structure and Chlorophyll Content in Wheat Coleoptiles. *Biol. Plant.* **1978**, *20* (6), 440–445.

(45) Foyer, C. H.; Noctor, G. Redox Sensing and Signalling Associated with Reactive Oxygen in Chloroplasts, Peroxisomes and Mitochondria. *Physiol. Plant.* **2003**, *119* (3), 355–364.

(46) Bari, R.; Jones, J. D. G. Role of Plant Hormones in Plant Defence Responses. *Plant Mol. Biol.* **2009**, *69* (4), 473–488.

(47) Vandenbroucke, K.; Robbens, S.; Vandepoele, K.; Inzé, D.; Van de Peer, Y.; Van Breusegem, F. Hydrogen Peroxide–Induced Gene Expression across Kingdoms: A Comparative Analysis. *Mol. Biol. Evol.* **2008**, *25* (3), 507–516.

(48) Zhou, L.; Wang, X.; Shin, H.-J.; Wang, J.; Tai, R.; Zhang, X.; Fang, H.; Xiao, W.; Wang, L.; Wang, C.; Gao, X.; Hu, J.; Zhang, L. Ultrahigh Density of Gas Molecules

Confined in Surface Nanobubbles in Ambient Water. *J. Am. Chem. Soc.* **2020**, *142* (12), 5583–5593.

(49) Ghaani, M. R.; Kusalik, P. G.; English, N. J. Massive Generation of Metastable Bulk Nanobubbles in Water by External Electric Fields. *Sci. Adv.* **2020**, *6* (14), eaaz0094.

Table of Contents

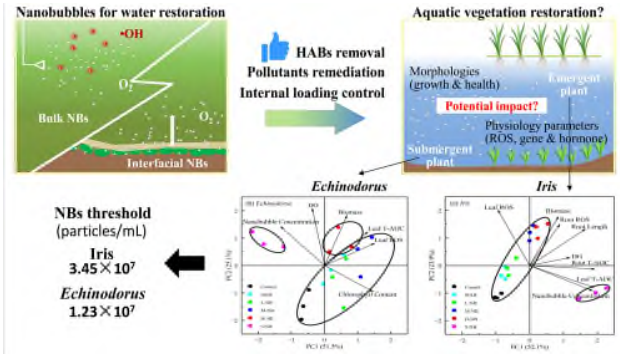

https://dspace.org/

Aquatic macrophytes in morphological and physiological responses to the nanobubble technology application for water restoration

Wang, Shuo; Liu, Yunsi; Lyu, Tao; Pan, Gang; Li, Pan

2020-12-04
American Chemical Society
https://doi.org/10.1021/acsestwater.0c00145
Wang S, Liu Y, Lyu T, et al., (2020) Aquatic macrophytes in morphological and physiological responses to the nanobubble technology application for water restoration. ACS ES&T Water, Volume 1, Issue 2, December 2020, pp. 376-387

Downloaded from a DSpace repository. https://dspace.org/